



## Discovery of novel inhibitors of *Trypanosoma cruzi trans-sialidase* from in silico screening

João Neres <sup>a,\*†</sup>, Mark L. Brewer <sup>b</sup>, Laura Ratier <sup>c</sup>, Horacio Botti <sup>d</sup>, Alejandro Buschiazzo <sup>d,e</sup>, Philip N. Edwards <sup>a</sup>, Paul N. Mortenson <sup>b</sup>, Michael H. Charlton <sup>b</sup>, Pedro M. Alzari <sup>e</sup>, Alberto C. Frasch <sup>c</sup>, Richard A. Bryce <sup>a,\*</sup>, Kenneth T. Douglas <sup>a</sup>

<sup>a</sup> School of Pharmacy and Pharmaceutical Sciences, University of Manchester, Manchester M13 9PT, UK

<sup>b</sup> Evotec (UK) Ltd, 114 Milton Park, Abingdon OX14 4SA, UK

<sup>c</sup> Instituto de Investigaciones Biotecnológicas, Universidad Nacional de San Martín, CC 30, 1650 San Martín, Argentina

<sup>d</sup> Unit of Protein Crystallography, Institut Pasteur de Montevideo, 2020 Mataojo, Montevideo 11400, Uruguay

<sup>e</sup> Dept de Biologie Structurale & Chimie, Institut Pasteur, 25 rue du Dr. Roux, 75724 Cedex 15 Paris, France

### ARTICLE INFO

#### Article history:

Received 12 November 2008

Revised 15 December 2008

Accepted 16 December 2008

Available online 24 December 2008

#### Keywords:

trans-Sialidase

Inhibitors

Virtual screening

*Trypanosoma cruzi*

Chagas disease

### ABSTRACT

*trans*-Sialidase from *Trypanosoma cruzi* (TcTS) has emerged as a potential drug target for treatment of Chagas disease. Here, we report the results of virtual screening for the discovery of novel TcTS inhibitors, which targeted both the sialic acid and sialic acid acceptor sites of this enzyme. A library prepared from the Evotec database of commercially available compounds was screened using the molecular docking program GOLD, following the application of drug-likeness filters. Twenty-three compounds selected from the top-scoring ligands were purchased and assayed using a fluorimetric assay. Novel inhibitor scaffolds, with  $IC_{50}$  values in the submillimolar range were discovered. The 3-benzothiazol-2-yl-4-phenyl-but-3-enoic acid scaffold was studied in more detail, and TcTS inhibition was confirmed by an alternative sialic acid transfer assay. Attempts to obtain crystal structures of these compounds with TcTS proved unsuccessful but provided evidence of ligand binding at the active site.

© 2008 Elsevier Ltd. All rights reserved.

The protozoan parasite *Trypanosoma cruzi* is the causative agent of Chagas disease, also known as American trypanosomiasis, transmitted to humans by haematophagous bugs and also directly by transfusion of infected blood. Chagas disease is widely distributed in Central and South America with 7.7 million persons currently infected and is estimated to cause 12,500 deaths annually, according to the World Health Organization.<sup>1</sup> The only established drugs for the acute phase of infection are nifurtimox and benznidazole, and there are no drugs capable of effectively treating the disease in the chronic stage. There has been considerable interest in developing novel approaches and targets for anti-*T. cruzi* drug design.<sup>2,3</sup> One of the targets discussed as a possible entry to novel therapeutics against Chagas disease is *trans*-sialidase (TcTS).<sup>4–6</sup> This enzyme plays a key role in the ability of

the parasite to evade the host immune response, mainly by transferring sialic acid residues from host glycoconjugates to the parasite surface.<sup>7,8</sup>

The mechanism of action of TcTS has been clarified both by kinetic and structural analysis, which provided evidence for a bisubstrate ping pong mechanism, with acid/base catalysis and formation of a covalently bound TcTS-sialosyl intermediate, via Tyr342.<sup>9,10</sup> The active site of TcTS exhibits some conserved features of microbial sialidases, including the presence of an arginine triad (Arg35, 245 and 314) that interacts with the negatively charged carboxylate group of sialic acid. The main difference from other sialidases is the presence of a second site, defined by two key residues (Tyr119 and Trp312), which accommodates the lactosyl moiety of donor and acceptor substrates, and is crucial for the *trans*-sialidase activity (in contrast with strictly hydrolytic sialidases).<sup>10</sup>

Despite the reported importance of TcTS for the pathogenesis of Chagas disease and its emergence as a potential drug target, inhibition of this enzyme has proved challenging, with no known strong, specific chemical inhibitors of TcTS.<sup>5</sup> The structures of representative TcTS inhibitor classes previously described in the literature are shown in Figure 1, with the respective inhibition constants. TcTS inhibitors can be grouped in two broad categories, namely sialic acid mimetics, which essentially target the sialic acid

**Abbreviations:** TcTS, *trans*-sialidase; DANA, 2-deoxy-2,3-didehydro- $\alpha$ -N-acetylneuraminic acid; 4-Methylumbelliferyl- $\alpha$ -D-N-acetylneuraminic acid, MuNANA; TIA, *trans*-sialidase inhibition assay.

\* Corresponding authors. Tel.: +44 (0) 161 275 8345; fax: +44 (0) 161 275 2481 (R.A. Bryce).

E-mail addresses: [dealm002@umn.edu](mailto:dealm002@umn.edu), [jneres@hotmail.com](mailto:jneres@hotmail.com) (J. Neres), [Richard.Bryce@manchester.ac.uk](mailto:Richard.Bryce@manchester.ac.uk) (R.A. Bryce).

† Present address: Center for Drug Design, University of Minnesota, 516 Delaware St. SE, Minneapolis, MN 55455, USA.

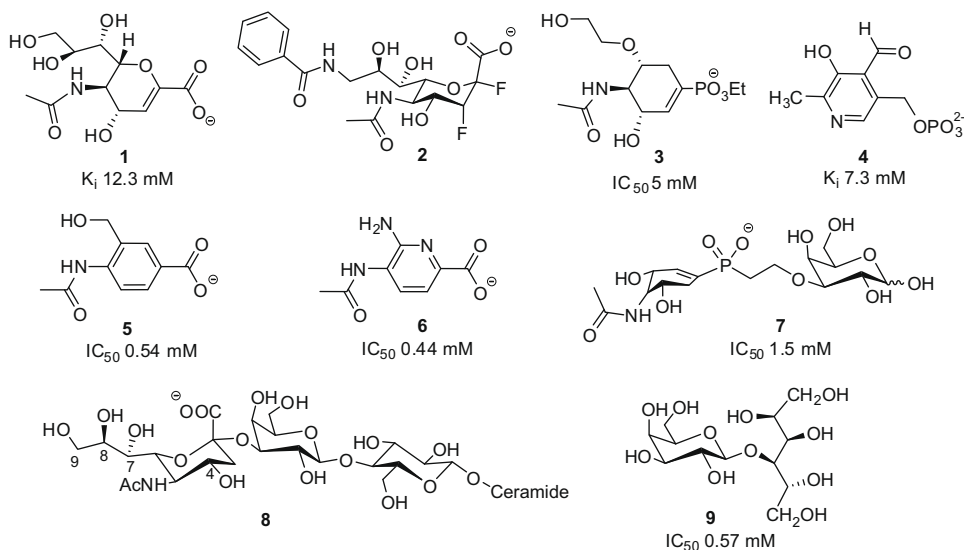


**Figure 1.** Structure and inhibition data for representative known TcTS inhibitors. See text for details on compounds **2** and **8**.

binding site (compounds **1–6**, Fig. 1) or sialic acid donor or acceptor substrates (**7–9**).<sup>5</sup>

2-Deoxy-2,3-didehydro-*D*-N-acetylneurameric acid (DANA, **1**, Fig. 1) is a potent transition state analogue inhibitor of the homologous enzyme Influenza neuraminidase but an extremely weak inhibitor of TcTS.<sup>11</sup> DANA analogues **3**, **5** and **6** exhibited improved, but still weak TcTS inhibition,<sup>12,13</sup> similar to the observed potency of pyridoxal phosphate **4**.<sup>14</sup> 2,3-Difluorosialic acid analogues such as **2** are mechanism-based TcTS inhibitors, which form a covalent bond with the hydroxyl group of Tyr342, but only at high concentrations (millimolar range).<sup>15</sup>

The most potent TcTS inhibitor known, resulting from modifications in the GM<sub>3</sub> ganglioside (**8**) and with  $IC_{50}$  values in the 10–100  $\mu$ M range,<sup>16</sup> fills in both sialic acid acceptor and donor sites. This result, together with the disappointing performance of sialic acid mimetics, shows the importance of the sialic acid acceptor site for TcTS inhibition. However, compounds such as lactitol (**9**) and its derivatives, which target this site only and are alternative sialic acid acceptors (by inhibiting the transfer of sialic acid to native acceptor substrates) were also disappointingly weak.<sup>17,18</sup> Therefore, it appears that the best strategy to inhibit TcTS would involve compounds that occupy both sialic acid and sialic acid acceptor binding sites. Efforts have been made in this direction by Streicher and coworkers<sup>19</sup> who synthesized **7** and several analogues, which however were only low millimolar TcTS inhibitors.

In order to find novel, alternative and simpler inhibitor scaffolds for TcTS, we used virtual screening methods to search libraries of commercially available screening compounds, using both sialic acid and sialic acid acceptor sites as targets for docking. The Evotec in-house supplier database, containing ~2.5 million unique structures from over 40 suppliers of chemical compounds was used to build a virtual screening library. Application of drug-likeness filters to remove compounds that fail Lipinski's rules<sup>20</sup> and substructure filters to remove undesirable functional groups (reactive groups, possible fluorescent moieties, known toxicophores), identified 1.5 million drug-like molecules. Three sets of molecules were selected from the drug-like set to form our library for virtual screening: 175,000 molecules with carboxylate or carboxylate isostere functionalities, a randomly selected set of 80,000 molecules, and a diverse set of 50,000 molecules. The diverse set was identified using Evotec's proprietary 'hole-filling' software, which uses a parallel implementation of a maximum-dissimilarity algorithm.<sup>21</sup> This software ensured that the diverse set of 50,000 compounds not

only avoided areas of chemical space occupied by the other two sets, but was also diverse within itself.

The 305,000-member virtual screening library was docked into the active site of TcTS (PDB code 1MS3<sup>22</sup>) using the GOLD molecular docking program.<sup>23</sup> This particular structure was selected because the side chain of Tyr119 is oriented in such a way that it can form stacking interactions with the acceptor substrate. Input conformations for docking were generated using Corina.<sup>24</sup> Ligand protonation states were generated using  $pK_a$  prediction software from ACD-Labs.<sup>25</sup> An in-house SVL script within MOE<sup>26</sup> was used to process the results and generate a protonation state appropriate to the calculated  $pK_a$  values at pH 7.0. Here, the sulfonamide amide group is assigned its deprotonated form; the associated experimental  $pK_a$  of around 5–7.5 reflects this weak acidity.<sup>27</sup> Docking calculations with GOLD were performed using default parameters for three times speed-up in conjunction with the GoldScore scoring function and an active site region defined by a sphere of radius 10 Å that was centred so that both sialic acid and sialic acid acceptor sites could be explored. Each molecule was docked 10 times and the top-ranked pose was retained for further analysis. A post-docking filtering strategy that used a combination of rescoring, protein-ligand interaction filters, and energy minimisation was adopted to short-list a practical number of molecules for visual inspection.

Rescoring of the docked poses was performed using CScore<sup>28</sup> but due to the lack of potent TcTS inhibitor molecules, it was not known which of the scoring functions might be expected to give enrichment for this target. However, a pilot study performed at Evotec using a neuraminidase crystal structure (PDB code 1F8B) had shown previously that PMFScore and a normalised sum of the FScore and GScore scoring functions were able to give enrichment for a set of known active compounds for this related target (Brewer, M. L.; Mortenson, P. N.; Charlton, M. H., unpublished work), and on this basis these same two functions were deemed suitable for the selection of molecules in the present TcTS virtual screen.

Our second selection strategy involved the application of filters to identify docked molecules that were capable of forming key interactions with residues in the TcTS active site. Specifically, hydrogen bonding interactions with Arg314, Arg245, Arg53, Asp96, Asp59 and hydrophobic interaction with Tyr312 and Tyr119 were considered (Fig. 2). These interaction filters were chosen on the basis of interactions that are commonly observed in

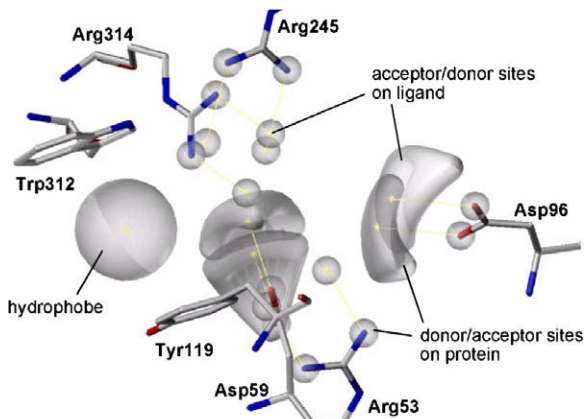


**Figure 2.** Key interactions observed in crystal structures of TcTS, used to develop interaction filters.

co-crystal structures of TcTS and were applied to the docked molecules here using Unity.<sup>29</sup>

Finally, the top ranked 5000 molecules according to both PMF and the normalised sum of FScore and GScore functions were combined with 5509 molecules that formed at least two of the key protein–ligand interactions to form a set of 14,945 unique molecules. This set was further profiled using an energy minimisation procedure that was implemented using a custom SVL script within MOE.<sup>26</sup> Briefly, each of the 14,945 docked molecules was energy minimised within the TcTS binding pocket ( $E_{\text{interaction}}$ ), and also within a continuum solvent model ( $E_{\text{ligand}}$ ), using the MOE implementation of the Amber94 force-field.<sup>30</sup> A binding energy was then associated with each compound as follows:  $E_{\text{bind}} = E_{\text{interaction}} - E_{\text{ligand}}$ .

The final numbers of molecules selected for inspection by the various strategies outlined above is summarised as follows: PMF-Score (300), normalised sum of FScore and GScore (300),  $\Delta E_{\text{bind}}$  (300), three key interactions (155) and two key interactions (900). Combining the five selections resulted in a set of 1819 unique compounds that was organised into 690 distinct clusters using a spectral clustering algorithm<sup>31</sup> to assess the level and representation of different chemotypes within the final set of virtual screening hit compounds. The post-docking filtering strategy was specifically designed to short-list compounds according to diverse criteria. However, it is perhaps surprising how little overlap was found between the chosen sets, particularly the sets that were identified with scoring functions. This may be partially attributed to the fact that each individual set only corresponds to a relatively small fraction of the entire docking virtual screening library that was used in the study.

The final stage of our selection process involved a visual inspection of the 1819 molecules in terms of both two-dimensional chemical structure and docked conformation in the TcTS active site. This resulted in a selection of 23 structurally diverse compounds that had at least one negatively charged functional group (carboxylate or sulfonamide) interacting with the arginine triad and, in most cases, a hydrophobic group placed between the side chains of Tyr119 and Trp312, filling the sialic acid acceptor binding site. This can clearly be observed in the docked conformation of compound **10** (Fig. 3) where the respective carboxylate group interacts well with the arginine triad, and the amide function hydrogen bonds with Arg245 and Asp59, thus providing additional stabilization of the triad. The thiophene ring is seen in the sialic acid acceptor binding site, and the benzene ring is positioned in the sialic acid site. The latter does not fill this site, thus introduction of functional groups could provide further interactions with key amino acid residues (e.g., Asp96, Gln195).

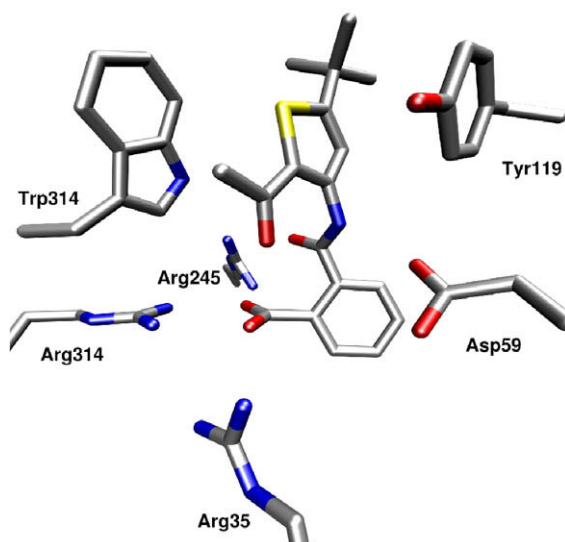


**Figure 3.** Docked pose of **10** showing interactions with key residues in the active site of TcTS and stacking interactions with Tyr119/Trp312.

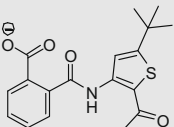
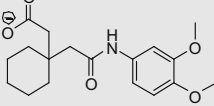
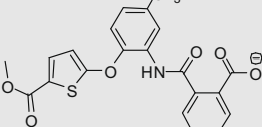
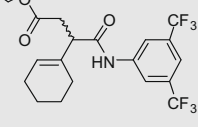
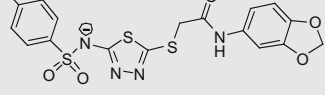
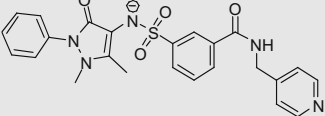
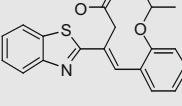
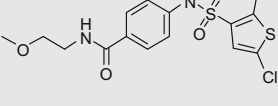
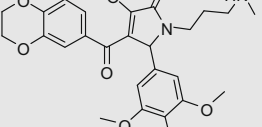
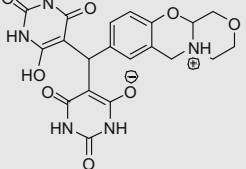
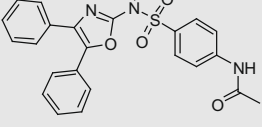
Selected compounds were purchased from Maybridge (Trevillet, Cornwall, UK), Enamine (Kiev, Ukraine), InterBioScreen (Moscow, Russia) and ChemDiv (Moscow, Russia). TcTS inhibition was primarily assessed using a continuous 96-well plate fluorimetric assay with recombinant TcTS and 4-methylumbelliferyl sialoside (MuNANA) as substrate, which measures sialic acid hydrolysis, as previously reported.<sup>32</sup> A 1 mM concentration of each compound, or the highest concentration permitted by its solubility, was initially screened in triplicate. Results obtained for the 21 compounds successfully tested (two compounds were not tested due to solubility issues) are shown in Table 1. Ten compounds were tested at concentrations below 1 mM, due to low aqueous solubility. Five compounds inhibited over 50% of the TcTS activity in the initial screening, and IC<sub>50</sub> values between 0.15 and 0.27 mM were determined for four of these (**10**, **15**, **17** and **27**) using the MuNANA fluorimetric assay (results shown in Table 1). Analysis of the structural features of these compounds shows that all are likely to be negatively charged in the protein active site at neutral pH, and none contains a positively charged group.

Considering the results obtained for the first set of selected compounds, we searched for analogues of the four best inhibitors in the MDL® Available Chemicals Directory (ACD database, MDL Information Systems Inc.). Several compounds containing the 3-benzothiazol-2-yl-4-phenyl-but-3-enoic acid scaffold of **17** but different phenyl ring substitution pattern were available. Seven of these were purchased to evaluate structure–activity relationship of this moiety (**32–38**). Similarly, **39**, an analogue of compound **10** was purchased. TcTS inhibition results are shown in Table 2 and were essentially identical for all the analogues, with measured IC<sub>50</sub>'s between 0.12 and 0.31 mM (analogues of **17**) or 0.29 for compound **39**. Selected compounds were also evaluated using an alternative assay, namely the *trans*-sialidase inhibition assay (TIA), which measures *trans*-sialidase activity using sialyllactose as sialic acid donor and <sup>14</sup>C-radioactively labeled lactose as acceptor.<sup>7,17</sup> Results from the TIA assay were similar to the observed with MuNANA, which further confirmed the inhibition of TcTS by compound **17** and its analogues.

The docked conformations obtained for compound **17** and its analogues (**32–38**) showed very similar results and confirmed the apparently good fitting of this structural family to the active site of TcTS. In all cases, the carboxylate group was positioned in close interaction with the arginine triad and the benzothiazole ring

**Table 1**

TcTS inhibition by purchased compounds selected from the virtual screening

Structure	MuNANA assay			TIA assay $IC_{50}$ (mM)	
	Screening		$IC_{50}$ (mM)		
	Concentration (mM)	% Inhibition			
	1.0	84	0.27	—	
	1.0	n.i.	—	—	
	1.0	21	—	—	
	1.0	32	—	—	
	1.0	82	0.28	—	
	1.0	23	—	—	
	1.0	92	0.15	0.29	
	1.0	50	—	—	
	0.5	41	—	—	
	0.5	28	—	—	
	0.125	22	—	—	

**Table 1** (continued)

n.i., no inhibition.

**Table 2**TcTS inhibition by analogue compounds to **10** and **17**

Structure	R	MuNANA assay		TIA assay	
		Concentration (mM)	% Inhibition	IC <sub>50</sub> (mM)	IC <sub>50</sub> (mM)
	<b>32</b>	1.0	91	0.31	—
	<b>33</b>	0.5	84	0.18	—
	<b>34</b>	1.0	94	0.12	—
	<b>35</b>	1.0	90	0.16	0.42
	<b>36</b>	1.0	91	0.12	—
	<b>37</b>	0.1	30	—	0.52
	<b>38</b>	1.0	92	0.15	—
	<b>39</b>	1.0	79	0.29	1.0 mM 32% inhibition

stacked between Tyr119 and Trp312 (Fig. 4A). However, a closer look at the phenyl ring of these compounds, positioned inside the sialic acid binding site, shows that no specific interactions were made in this region, except for compound **37** where the hydroxyl group appears hydrogen-bonded to Asp96. Comparison between the crystallographic conformation of sialyllactose (crystal structure 1S0I<sup>10</sup>) and the docked conformations of **17** and **35** (Fig. 4B) clearly shows that the phenyl rings in these structures are only partially occupying the sialic acid site, mainly in the region occupied by the glycerol chain of the latter. The similarity between these compounds could explain the relatively flat structure–activity relationship data obtained. Therefore, more significant structural modifications, for instance, by introducing more polar substituents in the phenyl ring or replacing it by a heterocyclic system could lead to activity improvements.

To gain insight on the type of inhibition exhibited by compound **17** we used the MuNANA fluorimetric assay in a discontinuous mode (described elsewhere).<sup>12</sup> The Lineweaver–Burk and Dixon plots of the data (Fig. 5) were compatible with both non-competitive and mixed inhibition models. Data fitting of the experimental data for compound **17** to the equations for these models by non-

linear least squares regression analysis using GRAFIT<sup>33</sup> afforded  $K_i$  values of 0.71 and 0.72 mM for the mixed inhibition model and 0.72 mM for the non-competitive model. This result shows the difficulty in distinguishing the two models in this case, as non-competitive inhibition is in fact a special case of mixed inhibition, occurring when the two  $K_i$  values are equal.<sup>34</sup> Similar behaviour has been observed for compound **5** (Fig. 1) which exhibited an inhibition potency in the same range as compound **17**.<sup>12</sup> The binding of **17** in locations distant from the catalytic site, despite having been discovered in a virtual screening directed to the active site, could be due to the relatively high concentrations necessary to achieve inhibition. We believe that structure-based improvement of **17** should lead to more potent TcTS inhibitors which should therefore exhibit increased specificity for the active site.

To evaluate and confirm the binding mode of compound **17** and its analogues **34**, **36** and **38** in complex to TcTS, we attempted to obtain co-crystal structures of TcTS, using conditions that had been successful for weaker TcTS inhibitors such as DANA.<sup>10,22</sup> These included soaking crystals of free TcTS with a solution of the compound in test, and also co-crystallization attempts of TcTS with compound concentrations up to 5 mM. In the particular case of compound **17**,

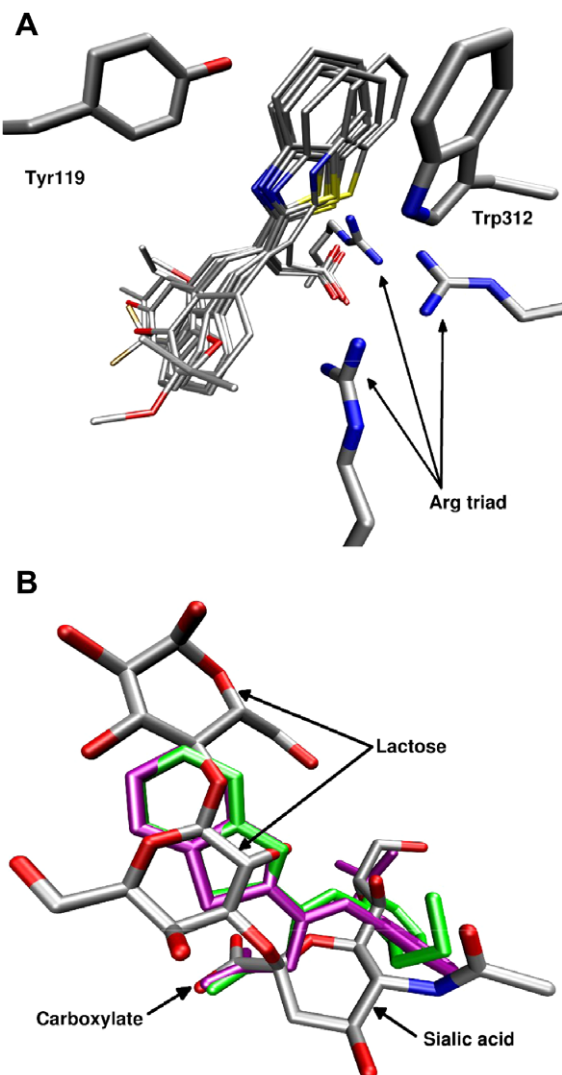


**Figure 4.** (A) Docked conformation of **17** and analogue structures (32–38) showing interactions with the arginine triad and the stacking interaction with Tyr119 and Trp312. (B) Docked structures of **17** (purple) and **35** (green) superimposed with the crystallographic conformation of sialyllactose (coloured by atom type, 1S01<sup>19</sup>). Hydrogen atoms are not shown.

co-crystallization attempts were unsuccessful, and soaking experiments generally resulted in dissolution of TcTS crystals, suggesting that this compound might be causing conformational changes that alter the crystal contacts. Lower concentrations of the inhibitor were used, diminishing crystal damage and allowing for X-ray diffraction data to be collected. The structure was solved at 1.7 Å, and after partial refinement ( $R_{\text{cryst}} 20.6\% / R_{\text{free}} 24.4\%$ ) evidence of the compound in the active site is observed (electron density features as well as the inhibitor-triggered Tyr119 displacement<sup>22</sup>). Unfortunately, the density was not clear enough to build an atomic model, most probably due to low occupancy. Extra peaks in difference Fourier maps were observed in a few sites distant from the reaction centre, in agreement with supplementary non-competitive inhibitor binding sites.

In summary, we performed an in silico screening experiment for the discovery of novel TcTS inhibitors, targeting both the sialic acid and sialic acid acceptor sites. Several filtering tools were employed to provide Lipinski rule-compliant compounds, remove undesirable functional groups and select compounds that could more likely inhibit TcTS. Evaluation of 23 purchased compounds using a fluorimetric assay resulted in the discovery of novel inhibitor

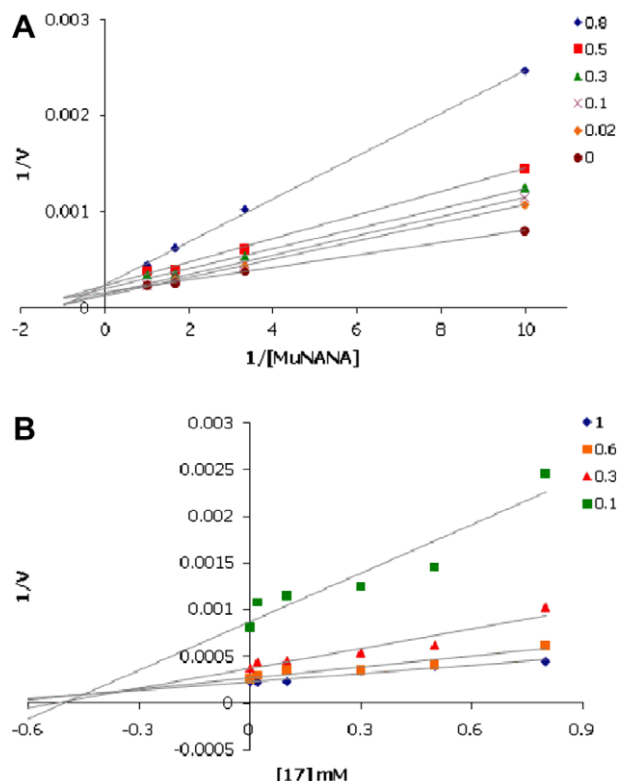


**Figure 5.** Graphical determination of the type of inhibition for compound **17**. (A) Lineweaver–Burk plot; (B) Dixon plot. Points are experimental; lines are by linear least squares regression analysis.

scaffolds, with  $IC_{50}$  values in the submillimolar range. Inhibition was confirmed for the most promising compound (**17**) and several of its analogues, by an alternative sialic acid transfer assay. Analysis of kinetic data from the MuNANA fluorimetric assay showed that **17** is most likely a non-competitive or mixed inhibitor. Attempts to obtain crystal structures of this compound with TcTS proved unsuccessful. Data gathered so far indicate that compound **17** seems to bind both in the active site and in other locations, distant from the active site. Further studies, namely of novel analogues of **17** specifically designed to improve interactions with the active site, would be necessary to confirm these assumptions, as more potent compounds that bind the active site would require lower concentrations for full inhibition, and reduce the likelihood of binding in alternative sites. More generally, the overall success of the approach presented in this article suggests that further virtual screening of the active site would be an efficient way to identify additional novel hit compounds which inhibit TcTS.

#### Acknowledgments

J.N. acknowledges financial support to the Portuguese Foundation for Science and Technology (F.C.T.). The work of A.C.F. was partially supported by an International Research Scholar Grant from the Howard Hughes Medical Institute.

#### References and notes

- Reporte sobre la enfermedad de Chagas, World Health Organization, Buenos Aires, Argentina, 2007.
- Schofield, C. J.; Jannin, J.; Salvatella, R. *Trends Parasitol.* **2006**, *22*, 583.
- Croft, S. L.; Barrett, M. P.; Urbina, J. A. *Trends Parasitol.* **2005**, *21*, 508.
- Buschiazzo, A.; Tavares, G. A.; Campetella, O.; Spinelli, S.; Cremona, M. L.; Paris, G.; Amaya, M. F.; Frasch, A. C. C.; Alzari, P. M. *EMBO J.* **2000**, *19*, 16.
- Neres, J.; Bryce, R. A.; Douglas, K. T. *Drug Discov. Today* **2008**, *13*, 110.
- Streicher, H. *Curr. Med. Chem.–Anti-inf. Agents* **2004**, *3*, 149.

7. Schenkman, S.; Jiang, M. S.; Hart, G. W.; Nussenzweig, V. *Cell* **1991**, *65*, 1117.
8. Ming, M.; Chuenkova, M.; Ortega-Barria, E.; Pereira, M. E. A. *Mol. Biochem. Parasitol.* **1993**, *59*, 243.
9. Damager, I.; Buchini, S.; Amaya, M. F.; Buschiazza, A.; Alzari, P.; Frasch, A. C.; Watts, A.; Withers, S. G. *Biochemistry* **2008**, *47*, 3507.
10. Amaya, M. F.; Watts, A. G.; Damager, T.; Wehenkel, A.; Nguyen, T.; Buschiazza, A.; Paris, G.; Frasch, A. C.; Withers, S. G.; Alzari, P. M. *Structure* **2004**, *12*, 775.
11. Paris, G.; Ratié, L.; Amaya, M. F.; Nguyen, T.; Alzari, P. M.; Frasch, A. C. *C. J. Mol. Biol.* **2005**, *345*, 923.
12. Neres, J.; Bonnet, P.; Edwards, P. N.; Kotian, P. L.; Buschiazza, A.; Alzari, P. M.; Bryce, R. A.; Douglas, K. T. *Bioorg. Med. Chem.* **2007**, *15*, 2106.
13. Streicher, H.; Busse, H. *Bioorg. Med. Chem.* **2006**, *14*, 1047.
14. Ferrero-Garcia, M. A.; Sanchez, D. O.; Frasch, A. C. C.; Parodi, A. J. *An. Asoc. Quim. Arg.* **1993**, *81*, 127.
15. Buchini, S.; Buschiazza, A.; Withers, S. G. *Ang. Chem.—Int. Ed.* **2008**, *47*, 2700.
16. Vandekerckhove, F.; Schenkman, S.; de Carvalho, L. P.; Tomlinson, S.; Kiso, M.; Yoshida, M.; Hasegawa, A.; Nussenzweig, V. *Glycobiology* **1992**, *2*, 541.
17. Agusti, R.; Paris, G.; Ratié, L.; Frasch, A. C. C.; de Lederkremer, R. M. *Glycobiology* **2004**, *14*, 659.
18. Agusti, R.; Giorgi, M. E.; Mendoza, V. M.; Gallo-Rodriguez, C.; De Lederkremer, R. M. *Bioorg. Med. Chem.* **2007**, *15*, 2611.
19. Busse, H.; Hakoda, M.; Stanley, M.; Streicher, H. *J. Carbohydr. Chem.* **2007**, *26*, 159.
20. Lipinski, C. A.; Lombardo, F.; Dominy, B. W.; Feeney, P. J. *Adv. Drug Deliv. Rev.* **1997**, *23*, 3.
21. Snarey, M.; Terrett, N. K.; Willett, P.; Wilton, D. *J. J. Mol. Graph. Model.* **1997**, *15*, 372.
22. Buschiazza, A.; Amaya, M. F.; Cremona, M. L.; Frasch, A. C.; Alzari, P. M. *Mol. Cell* **2002**, *10*, 757.
23. Jones, G.; Willett, P.; Glen, R. C.; Leach, A. R.; Taylor, R. *J. Mol. Biol.* **1997**, *267*, 727.
24. Corina 3.1, Molecular Networks GmbH, Erlangen, Germany, 2004.
25. pK<sub>a</sub> Batch, Advanced Chemistry Development Inc., Toronto, Canada, 2005.
26. MOE, Chemical Computing Group, Montreal, Canada, 2005.
27. Qiang, Z. M.; Adams, C. *Water Res.* **2004**, *38*, 2874.
28. Clark, R. D.; Strizhev, A.; Leonard, J. M.; Blake, J. F.; Matthew, J. B. *J. J. Mol. Graph. Model.* **2002**, *20*, 281.
29. Tripos, St. Louis, MO, USA, 2005.
30. Cornell, W. D.; Cieplak, P.; Bayly, C. I.; Gould, I. R.; Merz, K. M.; Ferguson, D. M.; Spellmeyer, D. C.; Fox, T.; Caldwell, J. W.; Kollman, P. A. *J. Am. Chem. Soc.* **1995**, *117*, 5179.
31. Brewer, M. L. *J. Chem. Inf. Model.* **2007**, *47*, 1727.
32. Neres, J.; Buschiazza, A.; Alzari, P. M.; Walsh, L.; Douglas, K. T. *Anal. Biochem.* **2006**, *357*, 302.
33. Grafit 5.0, 2005, Eritacus Software Ltd, Horley, Surrey, UK.
34. Cornish-Bowden, A. *Fundamentals of Enzyme Kinetics*; Portland Press Ltd: London, UK, 2004.